

ISSN: 2349-5162 | ESTD Year : 2014 | Monthly Issue

JOURNAL OF EMERGING TECHNOLOGIES AND INNOVATIVE RESEARCH (JETIR)

An International Scholarly Open Access, Peer-reviewed, Refereed Journal

Sensorless Control of BLDC Motor in Lopifit Treadmill Bicycle using Back EMF Observer **Estimation**

P. Devendra Naidu

dept. Electrical engineering Andhra university Visakhapatnam, India

Dr.P. Mallikarjuna Rao

dept. Electrical engineering Andhra University Visakhapatnam, India

Abstract— In this paper, the research investigates the implementation of sensorless control in a Lopifit treadmill bicycle, employing a Back EMF observer for precise control of a Brushless Direct Current (BLDC) motor. By eliminating the need for external sensors, this study aims to enhance the efficiency and reduce the complexity of the motor control system. The Back EMF observer estimation method is applied and evaluated, showcasing its effectiveness in achieving reliable and cost-effective motor control within the Lopifit platform. The Back EMF observer, a key component of this approach, estimates critical motor parameters such as rotor position and speed. It is possible to determine the position of the rotor using the proposed method, which models a trapezoidal back-EMF as an input and proposes a Back EMF observer that estimates a line-to-line back-EMF in real time. The fact that the information about a rotor position is calculated independently of the rotor speed without the use of an additional circuit or a laborious operation procedure is one particular way in which this observer performs well at low speeds. The proposed control scheme has been verified through simulations and experiments. The findings highlight the significance of sensorless control in enhancing the performance and accessibility of electricpowered transportation devices like the Lopifit treadmill bicycle.

Keywords—BLDC Motor, back - EMF Observer, Sensorless control, Rotor position, Rotor speed, Lopifit treadmill bicycle.

I. INTRODUCTION

The integration of electric propulsion systems in modern transportation devices has witnessed a remarkable surge, driven by the growing demand for sustainable and efficient mobility solutions. Among the various motor technologies, Brushless Direct Current (BLDC) motors have emerged as a preferred choice due to their high efficiency, compact size, and reliable operation. In this context, the Lopifit treadmill bicycle, a novel hybrid mobility solution, stands as a prominent example of innovative urban transportation. By combining the act of walking with the convenience of cycling, the Lopifit offers a unique and eco-friendly alternative for short-distance commuting

the effective operation of such hybrid mobility devices heavily relies on the performance of the integrated electric motor. Traditionally, sensor-based control systems have been employed to ensure precise motor control, providing feedback on critical parameters like rotor position, speed, and torque. However, this approach introduces complexities in system design, cost implications, and potential points of failure. To address these challenges, sensorless control techniques have gained prominence for their ability to achieve accurate control without the need for additional sensors.

Four groups can be made for traditional sensorless control techniques. A method for determining the conducting interval of freewheeling diodes connected in antiparallel with power transistors is the open phase current sensing method [3]. It has the benefit of a straightforward synchronous process and high performance at low speeds in the control characteristic. At high speeds, however, rotor position resolution noticeably degrades. This method specifically has the flaw that extra isolated power must be supplied to a comparator in order to detect the freewheeling current. Second, the technique for detecting the third harmonic of back-EMF [4,5] is a straightforward summation of three phase voltages that eliminates all fundamental and other polyphase components. The integration function performed on a signal with a frequency three times that of the fundamental signal has a reduced filtering requirement. Ultimately, the filter achieves high performance over a wide speed range, has a much smaller capacity than the flux detection method using back-EMF, and is not sensitive to filtering delays. To measure phase voltages, however, a neutral point that is not taken into account during the motor's manufacturing process is necessary. Additionally, at lowspeed ranges, third harmonics detection is challenging. Thirdly, the back-EMF integrating method [6,7] is a method that employs the idea that from Zero Crossing Point (ZCP) to 30, integration is constant. The main processor's workload is reduced as a result of the elimination of the need to compute an additional conversion point for the switching mode. This technique fails to synchronize the phase current at the sensorless device with the back-EMF. The flux-weakening drive is also not feasible. The open phase voltage sensing method [8-11] is a method for indirectly estimating the rotor position by using the ZCP detection of the terminal voltage of the open phase. It is the most popular type of sensorless control. This method must operate at a high operational speed in order to detect the ZCP of terminal voltages because its response degrades at transient states.

This research paper embarks on a comprehensive investigation into the sensorless control of a BLDC motor specifically tailored for the Lopifit treadmill bicycle. The primary focus is on the utilization of a Back Electromotive Force (EMF) observer estimation method. The Back EMF, an inherent property of BLDC motors, manifests as a voltage induced during commutation intervals and is directly proportional to the motor's speed. By accurately estimating this voltage, it becomes possible to infer crucial information about the motor's position and speed, thus enabling precise control without the need for external sensors.

II. MATHEMATICAL MODELLING OF BLDC **MOTOR**

A trapezoidal back-EMF type BLDC with 3 phases, 4 poles, and a Y connection is modeled. The term "trapezoidal back EMF" describes the shape of the mutual inductance between the stator and the rotor. Consequently, a b c phase D-Q axis is less practical than variable model. The Several presumptions are made, including: Magnetic circuit Saturation, Stator resistance, personal and interpersonal All phases have constant and equal inductance.

Fig. 1 displays the block diagram for the BLDC motor drive. The voltage equation for the three phases can be written as (1) [18] under the assumption that the stator resistances of all the windings are equal, as well as that self and mutual inductances are constant. Magnets, high resistivity stainless steel retaining sleeves, rotorinduced currents, and damper windings are not taken into account in this equation.

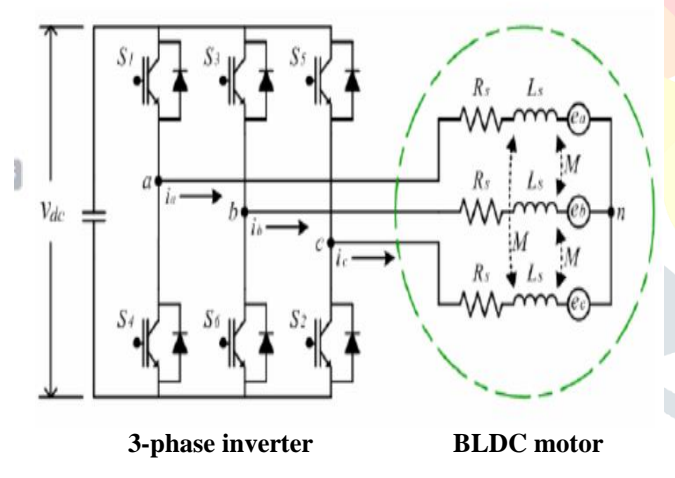


Fig 1: Block Diagram of a BLDC motor drive The BLDC's mechanical and electrical mathematical equations are as follows:

Equations for phase voltage in BLDC motor

$$V_{a} = Ri_{a} + (L - M) \frac{di_{a}}{dt} + E_{a} \dots (2.1)$$

$$V_{b} = Ri_{b} + (L - M) \frac{di_{b}}{dt} + E_{b} \dots (2.2)$$

$$V_{c} = Ri_{c} + (L - M) \frac{di_{c}}{dt} + E_{c} \dots (2.3)$$

Equations for back EMF in BLDC motor

$$E_a = K_a \omega_m F(\theta_a) \dots (2.4)$$

$$E_b = K_e \omega_m F(\theta_e - \frac{2\pi}{3}).....(2.5)$$

$$E_c = K_e \omega_m F(\theta_e - \frac{4\pi}{3}).....(2.6)$$

Equations for Torque/phase in BLDC motor

$$T_a = K_t i_a F(\theta_e) \dots (2.7)$$

$$T_b = K_t i_b F(\theta_e - \frac{2\pi}{3})....(2.8)$$

$$T_c = K_t i_c F(\theta_e - \frac{4\pi}{3})....(2.9)$$

From the above Equations

$$\begin{bmatrix} V_{a} \\ V_{b} \\ V_{c} \end{bmatrix} = \begin{bmatrix} R_{S} & 0 & 0 \\ 0 & R_{S} & 0 \\ 0 & 0 & R_{S} \end{bmatrix} \begin{bmatrix} i_{a} \\ i_{b} \\ i_{c} \end{bmatrix} + \begin{bmatrix} L_{S} - M & 0 & 0 \\ 0 & L_{S} - M & 0 \\ 0 & 0 & L_{S} - M \end{bmatrix} \frac{d}{dt} \begin{bmatrix} i_{a} \\ i_{b} \\ i_{c} \end{bmatrix} + \begin{bmatrix} e_{a} \\ e_{b} \\ e_{c} \end{bmatrix} ..(2.10)$$

The Electromagnetic torque for BLDC mo

$$T_{e} = T_{a} + T_{b} + T_{c}.....(2.11)$$

$$T_{e} = \frac{E_{a} i_{a} + E_{b} i_{b} + E_{c} i_{c}}{\omega_{m}}.....(2.12)$$

where the phase voltages are Va, Vb, and Vc. Stator resistance is denoted by Rs. Phase currents include ia, ib, and ic. The stator inductance is Ls. A mutual inductance is M. where L represents Ls - M moving forward. Phase back-EMFs are Ea, Eb, and Ec. A mechanical angle velocity is denoted by ωm.

III. PROPOSED SENSORLESS CONTROL METHOD

The proposed sensorless control method is based on the observation that the trapezoidal back-EMF of BLDC motors can be used to detect the rotor position. Since a BLDC motor's back-EMF cannot be measured directly, it must be inferred by an unknown input observer. The back-EMF, which is regarded as an unknown input and a state of the BLDC motor drive system, is used to build this unknown input observer. The following information can be obtained about the sensorless control method using an unknown input observer.

A. Using the unknown input observer, first line-to-line back-**EMF** estimation

Making the equation for one phase is challenging because the BLDC motor's neutral point is not provided. As a result, the following line-to-line equation takes into account the unknown input observer:

$$i_{ab} = -\frac{2R_s}{2L}i_{ab} + \frac{1}{2L}V_{ab} - \frac{1}{2L}E_{ab}....(2.13)$$

Iab and Vab are "known" state variables in (2.13) because they are measurably. However, since Eab cannot be measured, this term is regarded as a "UNKNOWN" state.

The Equation (2.13) can be rewritten in matrix form as:

x = Ax + Bu + Fw.....(2.14)y = Cx....(2.15)

where

$$A = \left[-\frac{2R_S}{2L} \right], B = \left[\frac{1}{2L2L} \right], F = \left[-\frac{1}{2L} \right]$$
$$x = \left[i_{ab} \right], u = \left[V_{ab} \right], w = \left[E_{ab} \right], y = \left[i_{ab} \right], C = [1]$$

Back-EMF is considered an unknown disturbance (2.14). Even the unknown disturbances, which typically have some variation of a step, ramp, or trigonometric function, are challenging to assume. Therefore, a differential equation can be used to model unknown disturbances:

$$z = Dz....(2.16)$$

 $w = Hz....(2.17)$

Where

$$D = \begin{bmatrix} \mathbf{0}_{(\delta-1)^*\mathbf{1}} & I_{(\delta-1)} \\ \mathbf{0}_{\mathbf{1}^*\mathbf{1}} & \mathbf{0}_{\mathbf{1}^*(\delta-1)} \end{bmatrix}, H = \begin{bmatrix} I_1 & \mathbf{0}_{\mathbf{1}^*(\delta-1)} \end{bmatrix}$$

In this I is Identity Matrix and δ is degree of polynomial under:

$$w = \sum_{i=0}^{\delta} a_i t^i, \delta \ge 1.....(2.18)$$

where ai stands for a group of unidentified coefficient vectors. Ai can be defined as ai = 0 in (2.18) when there is no experimental data on the disturbance. By increasing the degree of polynomial expression, this modeling technique provides an accurate model for the majority of disturbances as well as for unknown disturbances that change slowly. From this point forward, it is assumed without losing generality that the general fully observable dynamical system of (2.16, 2.17), models the unknown disturbance w. As a result, the augmented equation that introduces disturbances of differential equation form modeling the back-EMF can describe the entire system. It is possible to depict the augmented model as (2.19), and (2.20).

$$x_a = A_a x_a + B_a u$$
.....(2.19)
 $y = C_a x_a$(2.20)

where

$$A_{a} = \begin{bmatrix} A & FH \\ 0 & E \end{bmatrix} = \begin{bmatrix} -\frac{2R_{S}}{2L} & -\frac{1}{2L} \\ 0 & 0 \end{bmatrix}, x_{a} = \begin{bmatrix} i_{ab} \\ E_{ab} \end{bmatrix}$$

$$B_{a} = \begin{bmatrix} B \\ 0 \end{bmatrix} = \begin{bmatrix} \frac{1}{2L} \\ 0 \end{bmatrix}, u = \begin{bmatrix} V_{ab} \end{bmatrix}, y = \begin{bmatrix} i_{ab} \end{bmatrix}$$

$$C_{a} = \begin{bmatrix} C & 0 \end{bmatrix} = \begin{bmatrix} 1 & 0 \end{bmatrix}$$

And $\delta = 1$ determines the polynomial expression's degree of disturbance. Systems of (2.19) and (2.20) are observable, so the following observer can be created:

$$\hat{x}_a = A_a \hat{x}_a + B_a u + K(y - \hat{y})......(2.21)$$

K is the observer's gain matrix. If the observer's gain is properly chosen, it can calculate the line-to-line currents and back-EMFs of motors with high accuracy. A block diagram of the suggested back-EMF observer is shown in Fig. 3.

The equation for the entire observer, which includes all three phases, is as follows:

B. Commutation function

It is common practice to use sensorless control, which determines when switching devices will commutate by detecting the ZCP of the back-EMF. However, at low speeds, this method is unable to detect ZCP. The sensitive commutation function, which is defined using the line-to-line back-EMF observer, is proposed as a solution to this issue in order to enhance the performance of the sensorless control scheme depicted in Fig. 4.

The commutation functions (CF) are defined as follows:

Mode 1 and 4:
$$CF(\theta)_1 = \frac{\stackrel{\frown}{E_{bc}}}{\stackrel{\frown}{E_{ca}}}.....(2.23)$$

Mode 2 and 5:
$$CF(\theta)_2 = \frac{\stackrel{\wedge}{E_{ab}}}{\stackrel{\wedge}{E_{ba}}}.....(2.24)$$

Mode 3 and 6:
$$CF(\theta)_3 = \frac{\stackrel{\frown}{E_{ca}}}{\stackrel{\frown}{E_{ab}}}.....(2.25)$$

According to Fig. 4, the fractional equation consisting of a denominator () that gradually decreases and a numerator () that has a constant negative magnitude represents the commutation function for the mode conversion from mode 6 to 1. This commutation function abruptly switches from negative to positive infinity prior to mode change, and this moment is regarded as the position signal so that this feature can be positively separated from noises by choosing an appropriate threshold magnitude. The commutation functions of the proposed scheme have the property of being less noise sensitive, despite the fact that a similar commutation function has been reported [20].

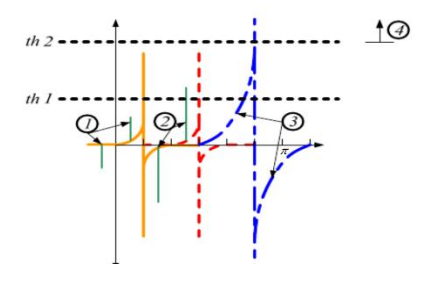


Fig 2: Commutation function using the existing method

The proposed commutation function and the current commutation function are shown in Figs. 5 and 6, respectively. In Fig. 5, the rotor's position can be detected without being affected by noise below the threshold (th1), but noise above the threshold (th1) can be viewed as a commutation signal and cause rotor position errors. Additionally, the th voltage level should be raised to achieve the precise commutation signal in the case of commutation functions like 3 caused by variations in the back-EMF, just as in the event that noise 2 is present.

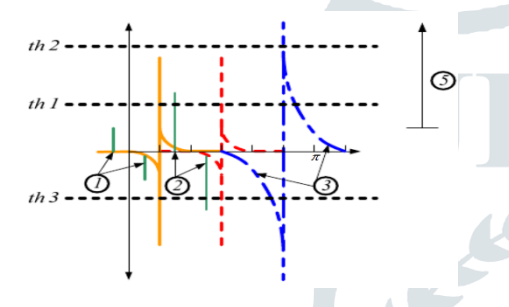


Fig 3: Commutation function using the proposed method

The bigger signal than th 1 or th 3, such as 2 and 3, are not taken into account in the proposed method because they are generated at a point before negative infinity. Instead, the signal after passing negative infinity (th 3) and satisfying the bigger magnitude than th 1 is taken into consideration as the commutation signal, as shown in Fig. 6. Finally, because it must choose a higher voltage level th than th 2, the existing method is noise-sensitive and the calculation of the commutation point may be delayed. However, the suggested method can produce precise position data at lower voltage levels, like 5.

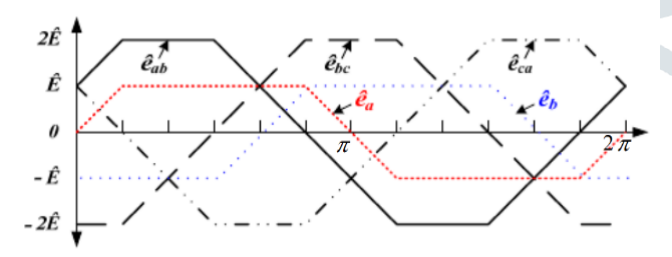


Fig 4: Relation between the Estimated back- EMFs and Line to Line back-EMF methods.

3.3. The Estimation of Position and Speed

Simple arithmetic can be used to determine the rotor position and speed if the estimated magnitude of a back-EMF is known. In BLDC motors, the following relationship exists between the speed and the size of a back-EMF:

$$E = K_a \omega_a(2.26)$$

where we is the electrical angular velocity, Ke is the back-EMF constant, and is the back-EMF magnitude.

According to Fig. 7, the maximum magnitude of the line-to-line back-EMF offered by the unknown input observer is used to estimate the back-EMF's magnitude. As a result, the speed can be determined using the back-EMF's estimated magnitude as follows:

$$\hat{\omega}_e = \frac{\hat{E}}{K_e}....(2.27)$$

$$\hat{\omega}_m = \frac{2}{P}\hat{\omega}_e....(2.28)$$

where P is the number of poles and ωm is an estimated mechanical angular velocity. Integrating the motor speed yields the rotor position:

$$\hat{\theta} = \int \hat{\omega}_e dt + \theta_0 \dots (2.29)$$

Where θm is the Rotor initial position.

3.4. Starting Procedure

The process must start in sensorless control because it struggles to determine the rotor position when at a standstill. The starting procedure for the proposed scheme has been adopted from the straightforward "align and go" scheme [3], which is a widely used technique in commercialized BLDC sensorless controller. In this method, the controller first conducts two phases of a motor before rotations to align the rotor with a predetermined position, and then rotates the rotor in accordance with a specified switching sequence while adjusting the rotor speed. Since they require a high enough speed to reach a specific level of voltage signals, closed loop control in traditional sensorless methods like detecting the ZCP of terminal voltages starts from a relatively high speed.

The interval between commutation points.

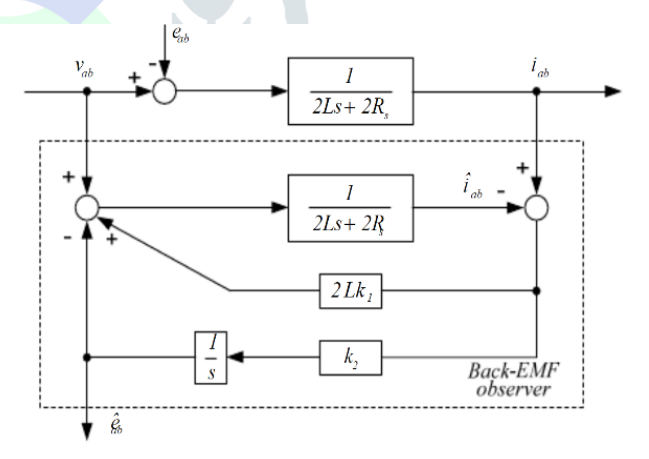


Fig 5: Proposed sensorless scheme block diagram

3.5. The overall block diagram of the Proposed sensorless scheme

The overall layout of the suggested sensorless drive system is shown in Fig. 8. Based on the DC-link voltage and the inverter's switching condition, the line-to-line voltage is calculated. The estimated line-to-line back-EMF (2.22) is provided by the back-EMF observer as previously mentioned. The estimated line-toline back-EMFs are used to calculate the commutation function (2.23-2.25), speed (2.28) and rotor position (2.29). Based on the calculated rotor position and the commutation function, the commutation signal generation block produces commutation signals. The hysteresis current controller uses commutation signals to regulate each phase current.

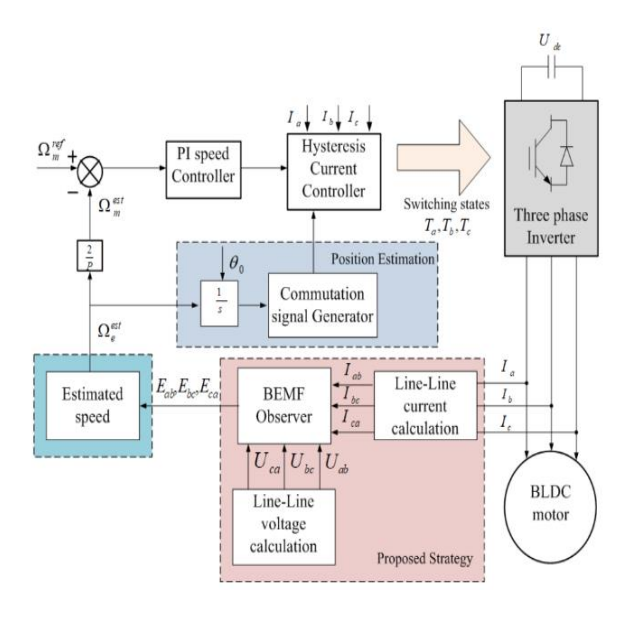


Fig 6: Structure of proposed sensorless drive system

IV. SIMULATION RESULTS

On the BLDC motor with the ratings and parameters listed in Table 1 simulations have been run. The simulations were performed in the MATLAB/Simulink environment.

Rated voltage	V	48 (V)
Rated torque	T_{e}	1.5 (Nm)
Rated speed	N_{r}	1600 (RPM)
Stator resistance	R_s	7.3 (Ω)
Stator inductance	L	0.02 (H)
Rotor inertia	$J_{\scriptscriptstyle m}$	23.16*10 ⁻⁴
Back – EMF constant	K_e	0.25(V/rad/sec)
Number of pole pairs	P_n	2

Table 1: Parameters and Ratings of BLDC motor

This paper assesses the sensorless algorithm's robustness to changes in speed and load. To evaluate how the drive will behave dynamically under load disturbance.

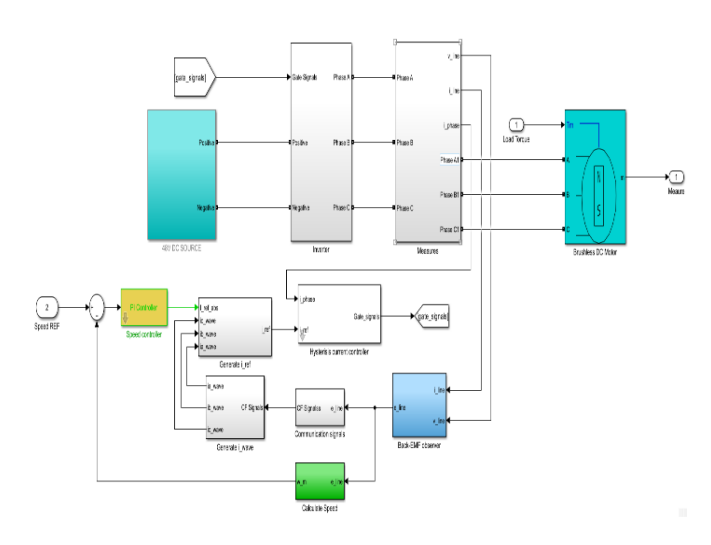
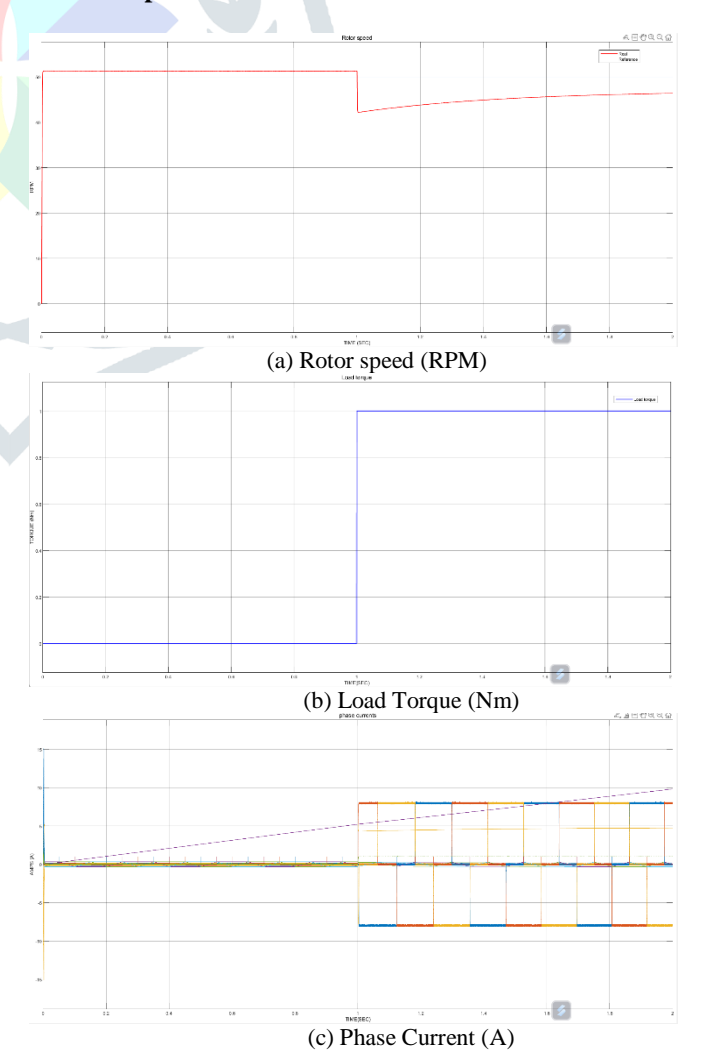


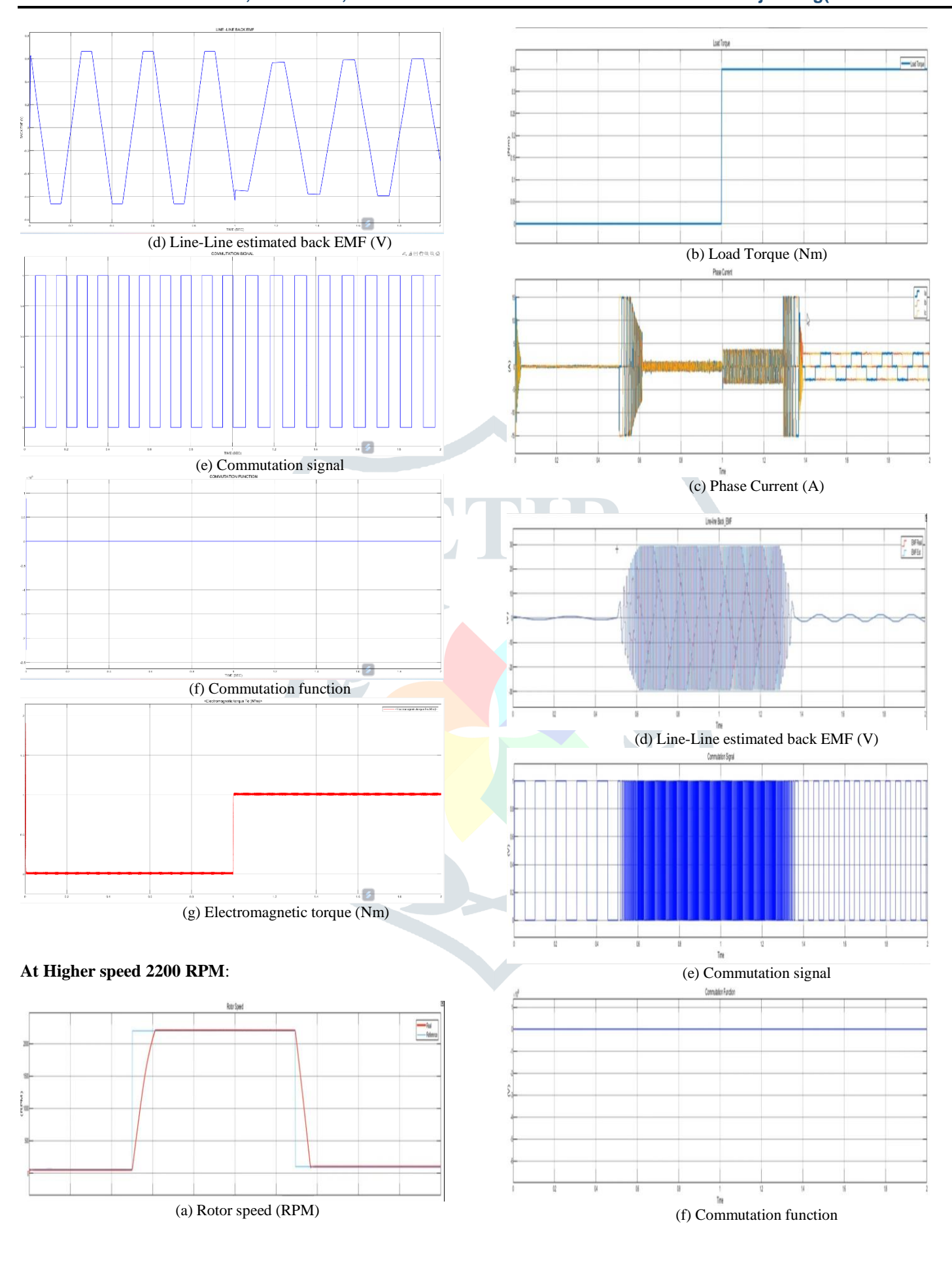
Fig 7: Simulation of the BLDC motor drive using proposed Sensorless scheme

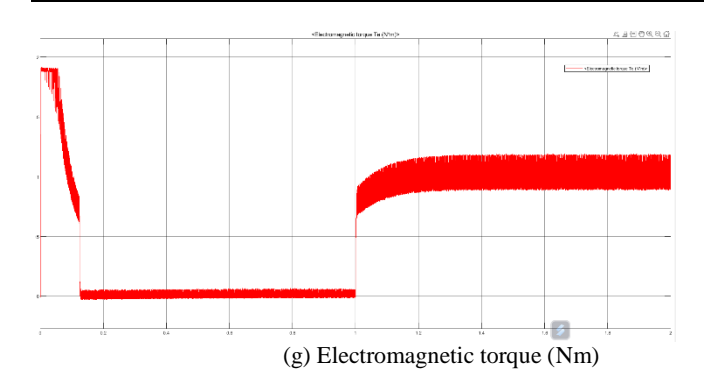
The simulation of sensorless control for Brushless Direct Current (BLDC) motors using Back Electromotive Force (EMF) observer estimation is a critical step in evaluating the effectiveness and robustness of this control strategy before its implementation in real-world applications. This process involves creating a virtual environment that mimics the behavior of a BLDC motor and assessing how the observer accurately estimates the Back EMF, rotor position, and speed under various operating conditions.

We simulate the above block at two different speed regions i.e.., lower and higher speeds as shown below:

At lower speed 50 RPM:







V. CONCLUSION

In conclusion, this research paper demonstrates the successful application of sensorless control using a Back EMF observer in a Lop fit treadmill bicycle integrated with a BLDC motor. The study's findings validate the effectiveness of the Back EMF observer in accurately estimating critical motor parameters, enabling precise control without the need for external sensors. This approach not only simplifies the system design but also reduces cost and potential points of failure. The experimental results showcase the robustness of the observer-based control system under varying operating conditions, highlighting its practical viability for real-world Lop fit applications. By leveraging the advantages of sensorless control, this research contributes to the advancement of efficient and cost-effective electric mobility solutions, with potential implications for a broader range of applications beyond Lop fit bicycles. The proposed methodology offers a promising avenue for enhancing the performance and accessibility of electric-powered vehicles in the evolving landscape of urban transportation. As a result, even in the transient state, it is possible to strictly estimate the actual rotor position and machine speed using the estimated line-to-line back-EMF.

The cutting-edge sensorless technique using a back EMF observer is to be

- be accomplished without using extra circuits.
- For precise control, determine the rotor speed in real time
- even in steady state and transient states, create a precise commutation pulse.
- effectively determine the rotor position over the entire speed range, particularly at low speeds.
- compute the commutation function using a noiseresistant method.
- be quickly implemented for industrial applications using a straightforward control algorithm.

The developed sensorless drive technique using the commutation function was successfully validated by simulation and experimental results.

6. REFERENCES

- N. Matsui, "Sensorless PM brushless DC motor drives," IEEE Trans. on Industrial Electronics, vol. 43, no. 2, pp. 300-308, 1996.
- 2. K. Xin, Q. Zhan, and J. Luo, "A new simple sensorless control method for switched reluctance motor drives," KIEE J. Electr. Eng. Technol., vol. 1, no. 1, pp. 52-57, 2006.
- 3. S. Ogasawara and H. Akagi, "An approach to position

- sensorless drive for brushless DC motors," IEEE Trans. on Industry Applications, vol. 27, no. 5, pp. 928-933, 1991.
- 4. C. Moreira, "Indirect sensing for rotor flux position of permanent magnet AC motors operating over a wide speed range," IEEE Trans. on Industry Applications, vol. 32, no. 6, pp. 1394-1401, 1996.
- 5. P. Pillay and R. Krishnan, "Modeling, simulation, and analysis of permanent-magnet motor drives, part II: The brushless DC motor drive," IEEE Trans. on Industry Applications, vol. 25, no. 2, pp. 274-279, 1989.
- 6. S. H. Huh, S. J. Seo, I. Choy, and G. T. Park, "Design of a robust stable flux observer for induction motors," KIEE J. Elect. Eng. Technol.,vol. 2, no. 2, pp. 280-285, 2007.
- 7. T. H. Kim and M. Eashani, "Sensorless control of the BLDC motors from near-zero to high speeds," IEEE Trans. on Power Electronics, vol. 19, no. 6, pp. 1635-1645, 2004.
- 8. A.Tashakori,M.Ektesabi,N.Hosseinzadeh,Modeling of BLDC Motor with Ideal BackEMF for Automotive Applications, Proceedings of the World Congress on Engineering (WCE), 2011, Vol II, London, U.K.
- 9. Electrical Motor Drives Modeling, Analysis and Control by R. Krishnan
- 10. Htet Htet Lwin, Nang Mwe Seng, Performance Comparison of P and PI Controller for Speed Control of Three Phase Brushless DC Motor, International Journal of Trend in Research and Development (IJTRD), Volume 5(5), ISSN: 2394-9333, Pp.358-360.
- Ming-Fa Tsai, Tran Phu Quy, Bo-Feng Wu, and Chung-Shi Tseng, Model Construction and Verification of a BLDC Motor Using MATLAB/SIMULINK and FPGA Control 6th IEEE Conference on Industrial Electronics and Applications, June 2011, Pp.1797-1802